



CHORUS

This is the accepted manuscript made available via CHORUS. The article has been published as:

Polyyne electronic and vibrational properties under environmental interactions

Marius Wanko, Seymour Cahangirov, Lei Shi, Philip Rohringer, Zachary J. Lapin, Lukas Novotny, Paola Ayala, Thomas Pichler, and Angel Rubio

Phys. Rev. B **94**, 195422 — Published 14 November 2016

DOI: [10.1103/PhysRevB.94.195422](https://doi.org/10.1103/PhysRevB.94.195422)

Polyynes Electronic and Vibrational Properties under Environmental Interactions

Marius Wanko,¹ Seymour Cahangirov,^{1,2} Lei Shi,³ Philip Rohringer,³ Zachary J. Lapin,⁴ Lukas Novotny,⁴ Paola Ayala,^{3,5} Thomas Pichler,³ and Angel Rubio^{1,6}

¹ Nano-Bio Spectroscopy Group and European Theoretical Spectroscopy Facility (ETSF), Universidad del País Vasco, CFM CSIC-UPV/EHU-MPC & DIPC, 20018 San Sebastián, Spain

² UNAM-National Nanotechnology Research Center, Bilkent University, 06800 Ankara, Turkey

³ University of Vienna, Faculty of Physics, 1090 Wien, Austria

⁴ ETH Zürich, Photonics Laboratory, 8093 Zürich, Switzerland

⁵ Yachay Tech University, School of Physical Sciences and Nanotechnology, 100119-Urcuquí Ecuador

⁶ Max Planck Institute for the Structure and Dynamics of Matter, Hamburg, Germany

Recently, the novel system of linear carbon chains inside of double-walled carbon nanotubes has extended the length of sp^1 hybridized carbon chains from 44 to thousands of atoms [L. Shi *et al.*, Nat. Mater. **15**, 634 (2016)]. The optoelectronic properties of these ultra-long chains are poorly described by current theoretical models, which are based on short chain experimental data and assume a constant environment. As such, a physical understanding of the system in terms of charge transfer and van der Waals interactions is widely missing. We provide a reference for the intrinsic Raman frequency of polyynes *in vacuo* and explicitly describe the interactions between polyynes and carbon nanotubes. We find that van der Waals interactions strongly shift this frequency, which has been neither expected nor described for other intramolecular C-C stretching vibrations. As a consequence of charge transfer from the tube to the chain, the Raman response of long chains is qualitatively different from the known phonon dispersion of polymers close to the Γ -point. Based on these findings we show how to correctly interpret the Raman data, considering the nanotube's properties. This is essential for its use as an analytical tool to optimize the growth process for future applications.

I. INTRODUCTION

Carbyne, the infinite sp^1 hybridized linear carbon chain, is often characterized by an intense Raman band associated with the eigenmode of the longitudinal-optical phonons of the conjugated polymer close to the Γ -point (called \mathfrak{A} -mode in Zerbi's effective conjugation coordinate theory^{1,2}). This Γ -mode vibration is characterized by an in-phase stretching of the chain's triple bonds. The current theoretical understanding of this material is founded on experimental data from colloidal sp^1 -carbon oligomers that are sterically stabilized by bulky end-groups. The longest chains of this type to date contain only 22 triple bonds ($N=44$ carbon atoms)³. The development of a novel system, long linear carbon chains stabilized inside double-walled carbon nanotubes (LLCCs@DWCNTs), has allowed for the synthesis of chains containing at least 8,000 carbon atoms⁴. These chains, which are long enough for proposed applications in composite materials⁵ and electronics⁶, are poorly described by current theory.

The electronic and vibrational properties of carbyne are greatly influenced by the local environment as has been observed for short polyyne chains in solution⁷⁻¹⁰, in CNTs¹¹⁻¹³, and on Ag surfaces⁸. Theoretical models for short colloidal chains show a softening of the Raman frequency that saturates at around $1,900\text{ cm}^{-1}$ ^{14,15}; however, Raman frequencies below $1,800\text{ cm}^{-1}$ have been observed for chains in double- and multi-wall CNTs¹⁶⁻¹⁸. We have now used scanning near-field optical spectroscopy to directly measure chain lengths and chain-band frequencies around $1,800\text{ cm}^{-1}$ for individual polyyne molecules of more than 1,000 atoms encapsulated in DWCNTs (inset in Fig. 1). The measured distribution of data points illustrates two basic limitations of scaling schemes and current empirical models. First, the empirical parameters are supposed to correct the unknown error of the DFT force

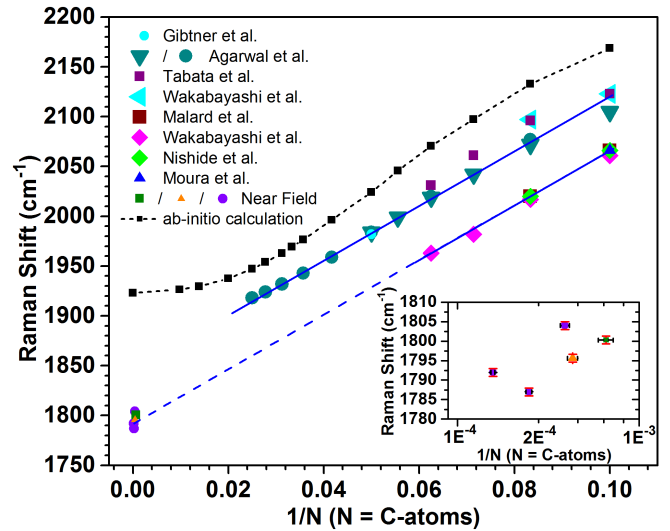


FIG. 1: Raman response of polyynes as a function of inverse length, given by the number N of carbon atoms. The solid lines are linear fits to the available data on chains with assigned lengths (upper solid line: colloidal chains⁷⁻¹⁰, lower solid line: chains inside CNTs¹¹⁻¹³, dashed blue line: extrapolation to infinite chains). The black dashed line shows theoretical SCS-MP2 results⁴. The inset shows data derived from near-field Raman microscopy images⁴.

field and account for unknown environmental interactions that are not included in the physical model. Second, they assume a specific and constant environment that does not vary with chain length. This may be valid in colloids but cannot represent a CNT environment with a distribution of tube chiralities that interact differently with the chain, depending on their physical diameter and electronic properties.

Previous experiments on the interaction of CNTs with short

chains of assigned length ($N=8-12$) have attributed the relative Raman shift, compared to colloidal chains, to charge transfer (CT) from the tube to the chain¹⁹. However, this conclusion was based on changes in the outer nanotube’s G-band red shift¹³, which can not be explained by a small CT alone, as the lifting of the Kohn anomaly by CT always leads a blue shift. Hence, this shift is most likely related to an internal strain inside the filled DWCNTs and not to a CT to the outer tubes.

Before Raman spectra of LLCCs@DWCNTs can be interpreted correctly and used for structural characterization, the following open questions must be answered: (1) To what extent are the LLCC@DWCNT spectra shifted by their local environment? (2) How does the variation in the measured frequencies depend on the nanotube chirality? (3) How does a specific medium affect the frequency softening for intermediate chain lengths ($N=50-100$ atoms), where *ab initio* calculations⁴ show a saturation (black curve in Fig. 1).

This work has two primary goals: (1) To obtain a reliable first-principles estimate of the Raman frequency of carbyne *in vacuo* using highly accurate coupled-cluster CCSD(T) calculations, which will provide a reference point for any environmental effects. (2) To illuminate the quantum nature of the tube–chain interaction. This is done in two parts by evaluating the effect of the van der Waals (vdW) interaction on the chain’s geometry and vibrational properties using an explicitly correlated method and the effect of CT between CNTs and carbon chains in the short- and infinite-chain limit using hybrid density functional theory. We find a surprisingly large and strongly length-dependent shift of the allowed Raman frequency of up to 280 cm^{-1} , which cannot be accounted for by CT alone. We show for the first time that vdW forces, which help to stabilize the chains inside the tube, modify the chain’s bond-length alternation (BLA). Due to this quantum effect, the polarizability of the environment directly affects the vibrational and optical properties of the chain in the combined system.

II. COMPUTATIONAL DETAILS

Hybrid DFT (PBE0 functional²⁰) and SCS-MP2 calculations were performed with the turbomole²¹ software (versions 6.1, 6.6, and 7.0). Finite C_NH_2 chains with N up to 102 were fully optimized at the SCS-MP2 level with turbomole, using a cc-pVDZ basis set. For N up to 40, the frequency of the resonant Raman active mode was calculated numerically. For $N>40$, we used the PBE0 eigenmodes to displace the SCS-MP2 geometry and generate a harmonic fit of the potential energy surface of SCS-MP2. This approach introduces an error of less than 1 cm^{-1} (for $N>20$) in the resulting frequency. The SCS-MP2 frequency for the infinite chain was obtained by a series of calculations of carbon rings (circular boundary condition). The ring size was increased up to 144 carbon atoms to achieve converged bond lengths and frequencies.

For the frequency calculations of the finite $C_{10}H_2$ chain *in vacuo* and inside SWCNT and DWCNT, we used the PBE and HSE functionals as implemented in the VASP 5.3.5 code²².

For the HSE functional, a range-separation parameter HF-SCREEN=0.2 was used. Like in the SCS-MP2 calculations, we employed the eigenmodes of gas-phase PBE0 calculations to obtain the force constants from the gradient of the displaced minimum-energy geometry. The following supercells and k -point samplings were used: 6-fold supercell of (10,0), (12,0), and (10,0)@(18,0) with 1 k -point and 9-fold supercell of (6,6) with 1 k -point.

For the PBE band-structure calculations of the infinite chain inside a (10,0)@(18,0) DWCNT, we used a 3-fold supercell of the DWCNT, which hosts 10 chain atoms. We used the equilibrium bond lengths of the chain *in vacuo* as obtained with the HSE functional. We did not optimize the chain inside the tube, because the GGA functional does not properly describe the BLA and favours a cumulenic structure inside CNTs²³. The box size was adjusted to the chain geometry. 31 irreducible k -points were used.

For the C_8H_2 @graphene calculations, a saturated graphene sheet of 78 atoms was used (Fig. 3). The geometry was fully relaxed with turbomole using SCS-MP2 (cc-pVDZ basis set), or DFT [SV(P) basis set] using the PBE functional with dispersion corrections^{24,25} (Table S2). The eigenmodes from gas-phase PBE0 calculations were employed to obtain the force constant of the Γ -mode. For C_8H_2 *in vacuo*, the resulting errors were smaller than 1 cm^{-1} when compared with the frequency from the full analytical Hessian.

CCSD(T)/cc-pVDZ geometry optimizations were performed with turbomole version 7.0.2 using symmetry-adapted numerical gradients. CCSD(T) frequencies were obtained using the displacements of the SCS-MP2 eigenmodes or (for $N=20$) those of the PBE0 Hessian (see above).

Benchmark calculations (Table S1 in the Supplemental Material²⁶) for the geometry of $C_{12}H_2$ were performed with ORCA using the cc-pVDZ basis set, except for the functionals LC-PBE, M11, ω B97XD, BMK, HISS, tHCTh, and CAM-B3LYP, which were performed with Gaussian²⁷.

III. RESULTS AND DISCUSSION

A. Polyynes *in vacuo*

To date there are no experimental IR or Raman spectra available for carbon chains *in vacuo*. Therefore, only calculated spectra can currently serve as a reference point to quantify the environment effect in measured spectra. The accurate *ab initio* prediction of the BLA and Γ -mode frequency of polyynes is challenging and previous calculations are indeed inconsistent, ranging from cumulene to strongly alternated carbyne. The disagreement of *ab initio* methods for long chains is well understood and can be attributed to the deficiencies of (semi-)local density functionals or to the incomplete description of local (dynamic) and long-range (static) correlation and has been studied extensively for polyenes²⁸⁻³⁰. Arguably the most precise methods that avoid these deficiencies and are computationally feasible are the coupled-cluster CCSD(T) and the diffusion Monte Carlo methods. Here, we performed CCSD(T) calculations to obtain reference geome-

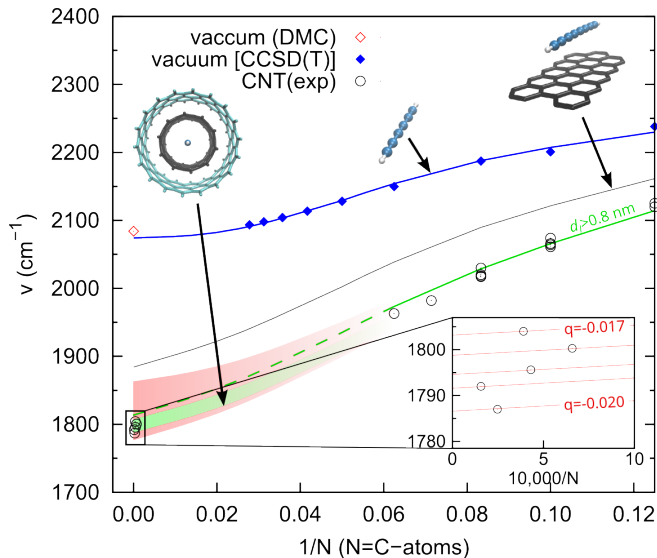


FIG. 2: Γ -mode frequency of C_NH_2 in different environments as a function of inverse chain length. The green area shows the effect of vdW interactions varying with the inner tube diameter d_I of a DWCNT within the range appropriate to host chains (0.65-0.75 nm). The solid/dashed green line represents the vdW interaction for larger d_I and is the closest match to the experimental data of short chains. The upper limit is the interaction with graphene ($d_I = \infty$, grey line). The red area shows the effect of a variable CT ranging from 0.010 to 0.022 e per chain atom (infinite chain) and decreasing with decreasing chain length. The inset shows the amount of CT (e per chain atom) required to reproduce the near-field Raman data, assuming the vdW shift associated with a constant d_I . Experimental data from refs.^{4,11-13}; diffusion Monte Carlo data (DMC) from Mostaani *et al.*³².

tries and vibrational frequencies for C_NH_2 with N ranging from 8 to 36. Our geometries are consistent with those of previous CCSD(T) calculations³¹ and our extrapolated BLA for the infinite chain is 0.125 Å, slightly less than obtained from diffusion Monte Carlo³² (see Fig. S1 in the Supplemental Material²⁶), and follows the same trend as polyenes³³. Longer chains are computationally unfeasible at the same level of theory and therefore we searched for the quantum chemical method that best reproduces the CCSD(T) data without scaling the force constants. Spin-component-scaled (SCS) variants of MP2³⁴ perform significantly better than any of the tested density functionals (see Table S1 in the Supplemental Material²⁶). The calculated SCS-MP2 frequencies are very accurate for short chains, but the slope is too large (Fig. S2). In order to extrapolate the CCSD(T) data to infinite chains, we scaled the SCS-MP2 data to fit the CCSD(T) points (blue line in Fig. 2). This yielded a Γ -point frequency for carbyne *in vacuo* of 2,075 cm^{-1} , very close to the diffusion Monte Carlo result by Mostaani *et al.*³² (red diamond in Fig. 2).

In Fig. 2 we compare the Γ -mode frequencies of chains *in vacuo*, as obtained from CCSD(T) theory, with experimental data from chains in CNTs. For the shortest chain, the Γ -mode frequency measured in a SWCNT is 118 cm^{-1} lower than *in vacuo* and the chain-length dispersion is differ-

ent. The frequency shift continuously increases to 187 cm^{-1} for $N=16$ and reaches remarkable 270-290 cm^{-1} for LLCCs@DWCNTs.

B. Chain length–tube chirality correlations

Assuming the growth conditions of LLCCs@DWCNTs allow the system to reach a thermal equilibrium distribution of chain lengths, it is clear that the average chain length must be different for each tube chirality as the tube–chain interaction energy depends on the physical inner tube diameter d_I ⁴. This is corroborated by the sub-peak structure of the LLCC Raman band^{4,16,35}. Moreover, the pressure-dependency of the sub-peaks³⁶ shows a direct dependence of the Raman shift on d_I , in addition to the shift from the nanotube’s electronic properties. Hence, the measured Raman frequencies cannot be described by one continuous $\nu(N)$ curve but rather a set of curves, each representing a specific tube diameter and chirality. This is illustrated in Fig. 2, where we use a simple empirical formula to model the N -dependent environment shifts due to vdW interactions and CT, based on experimental data and our calculations, as will be discussed below.

C. The effect of vdW interactions

The most common approach to describe dispersive or vdW interactions today is to add an atom-pair additive potential to the energy of a DFT calculation. It has been shown, though, that this ansatz can be quite inaccurate for low-dimensional systems due to many-body interactions and extended electron delocalization^{37,38}. The vdW interaction between molecular wires, for instance, changes drastically with their electronic properties³⁹⁻⁴¹. For the present system, the contribution of the vdW force to the tube–chain interaction energy can still be estimated with such additive potentials. Calculations of the direct effect of vdW interactions on the chain’s electronic, geometric and vibrational properties, in contrast, require methods that go beyond the pair-wise ansatz and have, to our knowledge, not been reported yet. Experiments, on the other hand, cannot easily distinguish it from competing physical effects such as CT and static polarization. Tentatively, vdW interactions have been associated with redshifts of the resonance energy of short chains inside SWCNTs^{13,19}. The observed trend, increasing redshift with CNT diameter, is surprising considering that the calculated interaction energy as a function of tube radius is largest in magnitude close to the vdW distance (3.3 Å) and decreases for larger diameters⁴. Moreover, when the tube diameter is reduced in high-pressure experiments, a redshift in the Raman frequency of the chain is observed³⁶.

Theoretically, it is clear that the parameters relevant for the vdW interaction, such as chain polarizability (α) and ionization potential (IP), depend on the chain’s BLA (see Fig. 5); however, it is impossible to correctly model the vdW interactions empirically based on such global properties alone (or their mapping onto atom-pair contributions) because the tube–chain separation is much smaller than the molecular

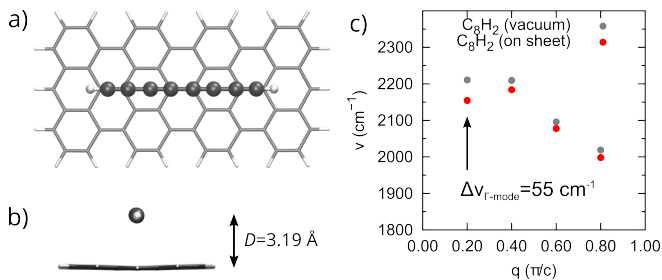


FIG. 3: Adsorption of a C_8H_2 chain on a graphene sheet. (a) Top view, (b) side view of the relaxed (SCS-MP2) geometry. (c) vibrational frequencies of the longitudinal optical phonons.

extension and the distance-dependency is highly non-trivial due to the strong coupling of inter- and intramolecular interactions. Novel approaches to capture this still widely unknown nonadditive behavior of vdW interactions have been proposed^{37,42–45}, but not tested for intramolecular vibrations yet. In particular, the importance of a self-consistent electronic Hamiltonian is unclear^{46,47}. Another approach is the “brute-force” *ab initio* calculation of the relevant electron correlation energy, which is computationally challenging and therefore limits the size of potential model systems.

As a minimal model that mimics a semiconducting tube of infinite diameter, we placed C_8H_2 on a hydrogen-terminated graphene sheet (Fig. 3) and calculated the fully relaxed geometry and vibrational spectrum. Indeed, the SCS-MP2 method predicts a reduced BLA and softening of the Γ -mode frequency by 55 cm^{-1} with respect to the isolated chain (Table S2 and Fig. 3). Comparative DFT-D calculations (Table S2), which reproduce the correct chain–sheet separation while neglecting the actual vdW correlation, show that other effects are small and do not significantly shift the vibrational frequency. Therefore, the length-dependent frequency shift due to the vdW interaction can be obtained as the difference between the total environment shift and the shift due to CT (*vide supra*). LLCCs are expected to exist in similar narrow inner tubes ($d_I=0.65\text{--}0.75 \text{ nm}$), which provide a maximal vdW interaction. The resulting frequency span is shown in Fig. 2 as green area.

D. The role of CT

Previous theoretical studies predicted a CT between carbyne and host tubes that reduces the BLA^{23,48}. To test whether CT is also relevant for short chains and can explain the observed red shift as compared to colloidal chains, we performed DFT calculations of $C_{10}H_2$ in different SWCNTs (Table I). We find only a small redshift ($21\text{--}25 \text{ cm}^{-1}$) for the Γ -mode in different tubes, consistent with a very small calculated CT from the tube to the chain. This result is not surprising as we find no hybridization between the chain and tube levels and the chain LUMO remains empty. Further, the effect of CT on the frequency may be overestimated by the PBE functional due to the above mentioned error in the phonon dispersion and slope of $\nu(N)$. This means that the redshift between

TABLE I: $C_{10}H_2$ *in vacuo* and in different CNTs.^a

	d_I	BLA	ν	$\Delta\nu$	Q_{chain}
vacuum		0.1040	2133	0	0.000
$C_{10}H_2@ (12,0)$	0.94	0.1038	2112	-21	-0.026
$C_{10}H_2@ (6,6)$	0.81	0.1034	2110	-23	-0.044
$C_{10}H_2@ (10,0)$	0.78	0.1035	2109	-24	-0.047
$C_{10}H_2@ (10,0)@ (18,0)$	0.78	0.1035	2108	-25	-0.056

^aPBE calculations of large supercells [6-fold for (m,0) and 9-fold for (6,6) tubes, see Computational Details for details]. Columns 2–6 show the (inner) tube diameter d_I (pm), BLA (\AA), Γ -mode frequency (cm^{-1}), shift with respect to vacuum (cm^{-1}), and net charge of the chain (e).

our CCSD(T) calculations ($2,201 \text{ cm}^{-1}$ *in vacuo*) and experimental data ($2,061 \text{ cm}^{-1}$ in SWCNT¹²) for $C_{10}H_2$ can not be accounted for by CT alone.

For long chains in double- or multi-wall CNTs the chain LUMO approaches the typical work function of these CNTs (Fig. S3), suggesting that the CT can be larger. We performed a DFT (PBE functional) supercell calculation of the infinite polyene chain (HSE vacuum geometry) inside a (10,0)@(18,0) DWCNT. Fig. 4 compares the band structures of the pristine and filled DWCNT. The chain LUMO band overlaps with the valence band of the metallic outer tube, which leads to a CT to the chain of $0.022 e$ per chain-atom. This CT is about one order of magnitude larger than that obtained for short chains and is comparable to the calculated inter-wall CT of DWCNTs⁴⁹.

The applied density functional, however, does not properly describe the BLA and phonon dispersion of the infinite chain. We therefore did not calculate these properties inside the DWCNT, but used the obtained CT as a parameter to estimate the effect on geometry and phonons in a smaller model system using more accurate methods. Fig. 5 shows the Raman frequencies of carbyne *in vacuo* and inside a (10,0) SWCNT as a functional of electron doping, which were calculated with the HSE hybrid functional and relaxed chain geometry. Inside the SWCNT, the excess charge localizes on the chain. Therefore, both calculations show nearly the same BLA and Γ -mode frequency for a given amount of charge. In agreement with earlier LDA calculations²³, the relation is clearly linear and the frequency redshifts by 176 cm^{-1} for a CT of $0.022 e$ per chain atom.

As also hybrid functionals overestimate the phonon dispersion (*vide supra*), we also performed SCS-MP2 calculations of the charged infinite chain (circular boundary conditions, see Computational Details). We obtained a frequency shift of 134 cm^{-1} for a CT of $0.022 e$ per chain atom. For both the hybrid DFT and the SCS-MP2 result, the frequency shift due to CT is clearly smaller than the total environment shift of 280 cm^{-1} . A major contribution must therefore arise from vdW interactions.

Even for a constant inner tube diameter and its associated vdW shift, the CT can vary with the electronic structure of the outer tube. The red area in Fig. 2 illustrates the frequency span resulting from a CT of $0.010\text{--}0.022 e$ per chain atom. The inset shows the amount of CT required to reproduce the experimental frequencies assuming a constant vdW interac-

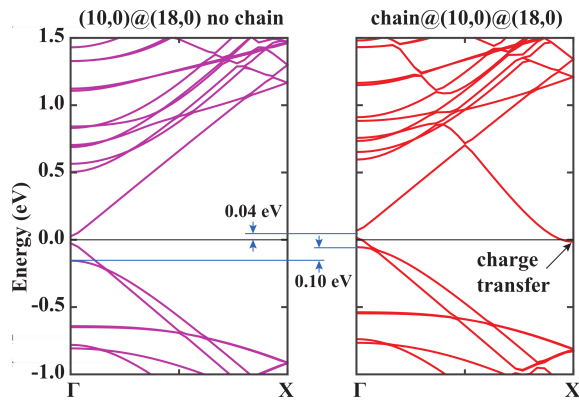


FIG. 4: Band structures of a (10,0)@(18,0) DWCNT empty (left) and encapsulating an infinite polyyne chain (right).

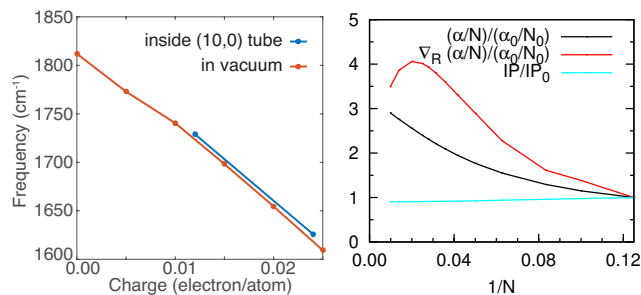


FIG. 5: Left: HSE calculation of the Γ -mode frequency of the infinite chain as a function of excess charge per chain atom. Right: Polarizability per C-atom, its derivative with respect to the displacement R along the Γ -mode, and IP. Properties are normalized with respect to C_8H_2 (α_0 , N_0 , and IP_0).

tion. Considering that the vdW interaction will increase with decreasing inner tube diameter, this range of CT can be seen as an upper limit. Raman data from short chains in CNTs is associated with larger tube diameters ($d_T > 0.9$ nm) and the gap between the tube's work function and the chain's LUMO is large. Hence, the frequency shifts in this range depend primarily on the chain length and the experimental data can be fitted by a single line in Fig. 2.

IV. CONCLUSIONS

In summary, our results show that long encapsulated chains interact with the nanotube in a way that qualitatively changes the Raman response and its dependence on the inverse chain length. The saturating behavior known from the phonon dispersion of polymers close to the Γ -point does not apply to these systems, which is a consequence of a variable CT and an unexpectedly strong effect of the van der Waals interaction. We have for the first time disentangled these two effects,

which strongly depend on the chain length and together shift the chain's Raman band by $118\text{-}290\text{ cm}^{-1}$.

The huge van der Waals shift, required to reproduce the Raman data of both short and long carbon chains, is also interesting from a theoretical point because currently no approaches exists that can describe it correctly for any realistic system. A comparison between a hypothetical polyyne and polyene dimer (Fig. S4) suggests that the high sensitivity of the C-C stretching frequency to van der Waals interactions might be a unique feature of extended systems that are close to a Peierls transition. This is inline with recent tight-binding calculations on carbyne-like chain dimers³⁸, which show that the power-law exponent that governs the asymptotic chain-chain interaction strongly depends on the ratio of the two different next-neighbor interaction parameters. These parameters reflect the BLA in the tight-binding model.

For ultra-long chains, i.e., confined carbyne, we predict an increased CT from the tube to the chain, which depends on the CNT's electronic properties. For the longest measured chains we estimate an upper limit of the CT of $0.02 e$ per chain atom, which varies by 15% depending on the tube chirality and accounts for about 40% of the shift. For short chains measured in wider CNTs the CT is smaller and causes shifts of $6\text{-}25\text{ cm}^{-1}$. Considering that both CT and vdW interactions depend on the tube chirality and that the equilibrium distribution of chain lengths is correlated with these tube properties, the limits of previous simple scaling schemes become obvious. On the other hand, our results show the pathway how to correctly assign the chain length from Raman spectroscopy. If additional information about the inner tube diameter and the electronic properties of the nanotube are considered, the chain's Raman band can be used as an analytic tool to optimize the growth of confined carbyne, which we see as an essential step towards accessing their theoretically outstanding application potential.

Acknowledgments

M.W. and A.R. acknowledge financial support by the European Research Council (ERC-2010-AdG-267374), Spanish MINECO (FIS2013-46159-C3-1-P), Grupos Consolidados (IT578-13), AFOSR Grant No. FA2386-15-1-0006 AOARD 144088, H2020-NMP-2014 project MOSTOPHOS (GA no. 646259), and COST Action MP1306 (EUSpec). Technical and human support provided by IZO-SGI (SGIker) of UPV/EHU. S.C. acknowledges financial support from the Marie Curie Grant FP7-PEOPLE-2013-IEF project ID 628876. T.P. acknowledges support from the Austrian Science Fund (FWF, NanoBlends I 943-N19). L.S. acknowledges the scholarship supported by the China Scholarship Council. Z.J.L. and L.N. acknowledge Swiss National Science Foundation (CR2212-152944).

¹ C. Castiglioni, J. T. L. Navarrete, G. Zerbi, and M. Gussoni, Solid State Commun. **65**, 625 (1988).

² B. Tian and G. Zerbi, J. Chem. Phys. **92**, 3892 (1990).

- ³ W. A. Chalifoux and R. R. Tykwinski, *Nat. Chem.* **2**, 967 (2010).
- ⁴ L. Shi, P. Rohringer, K. Suenaga, Y. Niimi, J. Kotakoski, J. C. Meyer, H. Peterlik, M. Wanko, S. Cahangirov, A. Rubio, et al., *Nat. Mater.* **15**, 634 (2016).
- ⁵ M. Liu, V. I. Artyukhov, H. Lee, F. Xu, and B. I. Yakobson, *ACS Nano* **7**, 10075 (2013).
- ⁶ R. H. Baughman, *Science* **312**, 1009 (2006).
- ⁷ T. Gibtner, F. Hampel, J. P. Gisselbrecht, and A. Hirsch, *Chem. Eur. J.* **8**, 408 (2002).
- ⁸ H. Tabata, M. Fujii, S. Hayashi, T. Doi, and T. Wakabayashi, *Carbon* **44**, 3168 (2006).
- ⁹ T. Wakabayashi, H. Tabata, T. Doi, H. Nagayama, K. Okuda, R. Umeda, I. Hisaki, M. Sonoda, Y. Tobe, T. Minematsu, et al., *Chem. Phys. Lett.* **433**, 296 (2007).
- ¹⁰ N. R. Agarwal, A. Lucotti, D. Fazzi, M. Tommasini, C. Castiglioni, W. Chalifoux, and R. R. Tykwinski, *J. Raman Spectrosc.* **44**, 1398 (2013).
- ¹¹ D. Nishide, T. Wakabayashi, T. Sugai, R. Kitaura, H. Kataura, Y. Achiba, and H. Shinohara, *J. Phys. Chem. C* **111**, 5178 (2007).
- ¹² T. Wakabayashi, T. Murakami, H. Nagayama, D. Nishide, H. Kataura, Y. Achiba, H. Tabata, S. Hayashi, and H. Shinohara, *Eur. Phys. J. D* **52**, 79 (2009).
- ¹³ L. G. Moura, C. Fantini, A. Righi, C. Zhao, H. Shinohara, and M. A. Pimenta, *Phys. Rev. B* **83**, 245427 (2011).
- ¹⁴ S. Yang, M. Kertesz, V. Zólyomi, and J. Kürti, *J. Phys. Chem. A* **111**, 2434 (2007).
- ¹⁵ A. Milani, M. Tommasini, and G. Zerbi, *J. Chem. Phys.* **128**, 064501 (2008).
- ¹⁶ A. Cupolillo, M. Castriota, E. Cazzanelli, L. Caputi, C. Giallombardo, G. Mariotto, and L. Papagno, *J. Raman Spectrosc.* **39**, 147 (2008).
- ¹⁷ M. Castriota, E. Cazzanelli, L. Caputi, A. Cupolillo, C. Giallombardo, L. Papagno, and G. Mariotto, *Diamond Relat. Mater.* **17**, 1716 (2008).
- ¹⁸ C. Zhao, R. Kitaura, H. Hara, S. Irlé, and H. Shinohara, *J. Phys. Chem. C* **115**, 13166 (2011).
- ¹⁹ L. G. Moura, L. M. Malaré, M. A. Carneiro, P. Venezuela, R. B. Capaz, D. Nishide, Y. Achiba, H. Shinohara, and M. A. Pimenta, *Phys. Rev. B* **80**, 161401 (2009).
- ²⁰ J. P. Perdew, M. Emzerhof, and K. Burke, *J. Chem. Phys.* **105**, 9982 (1996).
- ²¹ *TURBOMOLE V7.0 2015, a development of University of Karlsruhe and Forschungszentrum Karlsruhe GmbH, 1989-2007, TURBOMOLE GmbH, since 2007; available from <http://www.turbomole.com>.*
- ²² G. Kresse and D. Joubert, *Phys. Rev. B* **59**, 1758 (1999).
- ²³ Á. Ruzsnyák, V. Zólyomi, J. Kürti, S. Yang, and M. Kertesz, *Phys. Rev. B* **72**, 155420 (2005).
- ²⁴ S. Grimme, *J. Comput. Chem.* **27**, 1787 (2006).
- ²⁵ S. Grimme, J. Antony, S. Ehrlich, and H. Krieg, *J. Chem. Phys.* **132**, 154104 (2010).
- ²⁶ See Supplemental Material at <http://link.aps.org/supplemental/> for computational details and additional data.
- ²⁷ Gaussian 09, Revision D.01, M. J. Frisch, G. W. Trucks, H. B. Schlegel, G. E. Scuseria, M. A. Robb, J. R. Cheeseman, G. Scalmani, V. Barone, B. Mennucci, G. A. Petersson, H. Nakatsuji, M. Caricato, X. Li, H. P. Hratchian, A. F. Izmaylov, J. Bloino, G. Zheng, J. L. Sonnenberg, M. Hada, M. Ehara, K. Toyota, R. Fukuda, J. Hasegawa, M. Ishida, T. Nakajima, Y. Honda, O. Kitao, H. Nakai, T. Vreven, J. A. Montgomery, Jr., J. E. Peralta, F. Ogliaro, M. Bearpark, J. J. Heyd, E. Brothers, K. N. Kudin, V. N. Staroverov, T. Keith, R. Kobayashi, J. Normand, K. Raghavachari, A. Rendell, J. C. Burant, S. S. Iyengar, J. Tomasi, M. Cossi, N. Rega, J. M. Millam, M. Klene, J. E. Knox, J. B. Cross, V. Bakken, C. Adamo, J. Jaramillo, R. Gomperts, R. E. Stratmann, O. Yazyev, A. J. Austin, R. Cammi, C. Pomelli, J. W. Ochterski, R. L. Martin, K. Morokuma, V. G. Zakrzewski, G. A. Voth, P. Salvador, J. J. Dannenberg, S. Dapprich, A. D. Daniels, O. Farkas, J. B. Foresman, J. V. Ortiz, J. Cioslowski, and D. J. Fox, Gaussian, Inc., Wallingford CT, 2013.
- ²⁸ T. Körzdörfer, R. M. Parrish, J. S. Sears, C. D. Sherrill, and J.-L. Brédas, *J. Chem. Phys.* **137**, 124305 (2012).
- ²⁹ D. Jacquemin and C. Adamo, *J. Chem. Theory Comput.* **7**, 369 (2011).
- ³⁰ M. Wykes, N. Q. Su, X. Xu, C. Adamo, and J.-C. Sancho-García, *J. Chem. Theory Comput.* **11**, 832 (2015).
- ³¹ C. D. Zeinalipour-Yazdi and D. P. Pullman, *J. Phys. Chem. B* **112**, 7377 (2008).
- ³² E. Mostaani, B. Monserrat, N. D. Drummond, and C. J. Lambert, *Phys. Chem. Chem. Phys.* **18**, 14810 (2016).
- ³³ M. Barborini and L. Guidoni, *J. Chem. Theory Comput.* **11**, 4109 (2015).
- ³⁴ M. Gerenkamp and S. Grimme, *Chem. Phys. Lett.* **392**, 229 (2004).
- ³⁵ X. Zhao, Y. Ando, Y. Liu, M. Jinno, and T. Suzuki, *Phys. Rev. Lett.* **90**, 187401 (2003).
- ³⁶ N. Ferreira Andrade, A. L. Aguiar, Y. A. Kim, M. Endo, P. T. C. Freire, G. Bruneto, D. S. Galvao, M. S. Dresselhaus, and A. G. Souza Filho, *J. Phys. Chem. C* **119**, 10669 (2015).
- ³⁷ J. F. Dobson, *Int. J. Quantum Chem.* **114**, 1157 (2014).
- ³⁸ A. Ambrosetti, N. Ferri, R. A. DiStasio, and A. Tkatchenko, *Science* **351**, 1171 (2016).
- ³⁹ J. F. Dobson, A. White, and A. Rubio, *Phys. Rev. Lett.* **96**, 073201 (2006).
- ⁴⁰ R.-F. Liu, J. G. Ángyán, and J. F. Dobson, *The Journal of Chemical Physics* **134**, 114106 (2011).
- ⁴¹ V. V. Gobre and A. Tkatchenko, *Nat. Commun.* **4**, 2341 (2013).
- ⁴² Y. V. Shtogun and L. M. Woods, *J. Phys. Chem. Lett.* **1**, 1356 (2010).
- ⁴³ J. Klimes and A. Michaelides, *J. Chem. Phys.* **137**, 120901 (2012).
- ⁴⁴ R. A. DiStasio Jr, V. V. Gobre, and A. Tkatchenko, *J. Phys.: Condens. Matter* **26**, 213202 (2014).
- ⁴⁵ A. M. Reilly and A. Tkatchenko, *Chem. Sci.* **6**, 3289 (2015).
- ⁴⁶ N. Ferri, R. A. DiStasio, A. Ambrosetti, R. Car, and A. Tkatchenko, *Phys. Rev. Lett.* **114**, 176802 (2015).
- ⁴⁷ Y. Ikabata, T. Sato, and H. Nakai, *Int. J. Quantum Chem.* **113**, 257 (2013).
- ⁴⁸ A. Tapia, L. Aguilera, C. Cab, R. Medina-Esquivel, R. de Coss, and G. Canto, *Carbon* **48**, 4057 (2010).
- ⁴⁹ V. Zólyomi, J. Koltai, Á. Ruzsnyák, J. Kürti, Á. Gali, F. Simon, H. Kuzmany, Á. Szabados, and P. R. Surján, *Phys. Rev. B* **77**, 245403 (2008).